

# Experimental and Numerical Investigation of Gas-Liquid Flow in a Rectangular Bubble Column with Centralized Aeration Flow Pattern

Diana I. Sanchez-Forero<sup>a</sup>, João L. Silva Jr.<sup>a</sup>, Marcela K. Silva<sup>b</sup>, Jaci C.S.C.Bastos<sup>b</sup>, Milton Mori<sup>a,\*</sup>

<sup>a</sup>School of Chemical Engineering, University of Campinas, UNICAMP, Av. Albert Einstein, 500, CEP: 13083-970, Campinas, SP, Brazil

<sup>b</sup>Federal University of Maranhão - UFMA, Av. dos Portugueses, CEP: 65085-580, São Luís, MA, Brazil.  
 mori@feq.unicamp.br

Bubble columns are multiphase contact devices for mass and heat transfer, which are intensively used in different industrial areas. Flow and turbulence in these equipments are induced by bubble rise motion. In this work, the fluid dynamics of gas-liquid flow in rectangular bubble columns with centralized aeration were investigated via experiments and CFD simulations. Particle Image Velocimetry (PIV) experiments were performed in a rectangular bubble column, in order to obtain additional data of the flow field (axial velocity, turbulent kinetic energy and stress tensors) of continuous phase (liquid). The experimental results show typical axial mean velocity profiles of the liquid, upward flow in the core region and a down-flow near the wall. The Large Eddy Simulation predicted well the flow behaviour in the bubble column.

## 1. Introduction

Bubble columns serve as multiphase contactors and reactors in chemical, petrochemical, biochemical, and metallurgical industries. Excellent heat- and mass-transfer characteristics, lack of moving parts, higher durability of catalyst, ease of operation, compactness, and low operating and maintenance costs are the advantages that render bubble columns as an attractive reactor choice for various multiphase processes (Degaleesan et al., 2001). Despite the simplicity in mechanical design, fundamental properties of the two-phase fluid dynamics associated with the operation of a bubble column are still not fully understood because of the complex nature of multiphase flow (Dionísio et al., 2009). Gas-liquid systems operate by injection of the gas phase in the bottom of a column filled with liquid. This operation depends on several factors such as fluid physical properties, column dimension and inlet gas velocity (Silva et al., 2011).

In order to study the hydrodynamics of these equipments image techniques have been used to provide information on bubble and liquid velocity fields or bubble size distribution through the system (Bröder and Sommerfeld, 2007). Phase-Doppler, Laser-Doppler Velocimetry, acoustic techniques, Particle Image Velocimetry (PIV) and Particle Tracking Velocimetry (PTV) are some of these techniques (Bröder and Sommerfeld, 2009; Nogueira et al., 2003). However, methods to be used in experimental studies usually are limited to the visualization of the flow structure in bubble columns, then be need to carry out different techniques for detailed information about the structure of bubbly flow (Bröder and Sommerfeld, 2002).

PIV is a nonintrusive measurement technique that gives quantitative instantaneous whole-field velocity maps of the flow. This method use fluorescent tracers to seeding the liquid phase and allow the determination of velocity vectors close to the gas-liquid interface and to the wall (Nogueira et al., 2003). This paper presents a numerical and an experimental study of the two-phase homogeneous flow regime in rectangular bubble columns using CFD simulation and PIV technique in order to determine the fluid dynamic behaviour.

### 1.1 Case of Study

The experimental investigation consists in the study of two-phase homogenous flow in a rectangular bubble column for three different superficial gas velocities. The validation of theoretical calculations with Large Eddy Simulation approach for turbulence was performed using experimental data obtained by PIV technique. Mesh independence tests were achieved with approximately 120,000 control volumes. All the numerical simulation procedure was accomplished using the CFD commercial code ANSYS ICEM 14 (geometry and mesh generation) and CFX 14 (solver, pre and post processing).

## 2. Experimental Unit

### 2.1 Experimental facility

The experimental facility used is showed in Figure 1.

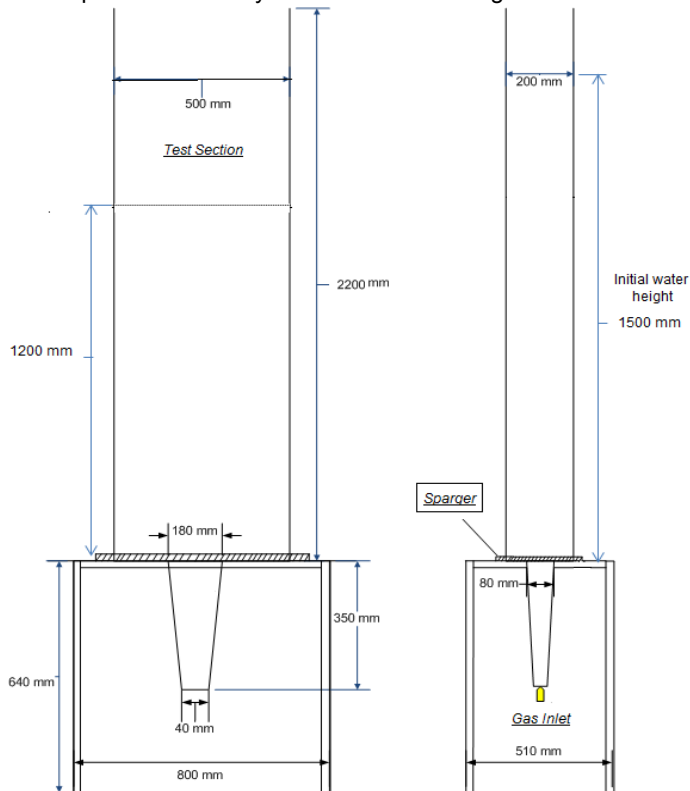


Figure 1: Experimental unit facility (front and side view of bubble column).

The laboratory bubble column is a rectangular transparent acrylic column of 0.5 m of width, 0.2 m of depth and 2.2 m of high, the gas feed is performed by 18 roles of 1 mm of inner diameter disposed in 3 rows in the central region of the column bottom. The operation consists in inject compressed air at the bottom of the column using the gas sparger. The air rises, forming bubbles which are distributed throughout the liquid domain. The liquid phase used in the experiments was distilled water. The measurements are performed at the top of the column at the distance of around 1.2 m of the injection section, with initial liquid height of 1.5 m.

### 2.2 PIV System in Homogeneous Bubble Flow

In order to collected 2500 double images to yield a continuous phase mean properties a CCD camera with a resolution of 1376 x 1024 pixel was used. This number of images was enough to obtain statistically reliable profiles for the continuous phase mean velocities. The images were transferred digitally from the CCD camera to the controlling and image processing PC. The axial component of the liquid velocities along the horizontal position at different superficial gas velocities ( $0.05 \text{ cm s}^{-1}$ ,  $0.09 \text{ cm s}^{-1}$  and  $0.13 \text{ cm s}^{-1}$ ) were measured using a PIV system.

The PIV images are obtained by seeding the liquid with fluorescents particles and illuminating it with a pulsed Nd:YAG laser with a wavelength of 532 nm. The tracer material was modified carboxi-acrylate

particles with fluorescent dye-rhodamine ( $C_{28}H_{31}N_2O_3Cl$ ) with a mean diameter of about  $15 \mu m$  and specific mass of  $1100 \text{ kg m}^{-3}$ . The time between the pulsing of the two laser cavities (pulse separation) is adjusted according to the measurement velocities at each test section (particle tracer motion approximately 5 pixels). The experimental operating conditions were shown in Table 1, where the  $\Delta t$  is the different between the first and the second photo.

Table 1: Experimental operating conditions

Gas superficial velocity ( $\text{cm s}^{-1}$ )	Initial liquid height (cm)	Axial level of data validation (cm)	$\Delta t$ ( $\mu s$ )
0.05			7,000
0.09	150	120	6,000
0.13			5,000

### 3. Mathematical Models

To describe the gas-liquid bubbly flow, the conservation of mass and momentum of each phase were solved by Navier-Stokes equations.

The Eulerian-Eulerian and Large Eddy Simulation approaches were used to account turbulence of continuous phase (liquid), using the Sub-Grid Scale model proposed by Smagorinsky, with a closure coefficient of 0.10. Drag and lift forces were considered for interphase momentum exchange, using Ishii and Zuber (1979) and Tomiyama (2004).

#### 3.1 Operating and Boundary Conditions and Numerical Mesh

The gas-liquid system is composed by air and water at  $25 \text{ }^\circ\text{C}$ . The column is opened to atmospheric pressure. No-slip condition was considered for both phases at column wall. For all cases were simulated 130 s (30 s for the flow stabilization + 100 s to provide the time-averaged results) with a time step of  $1 \times 10^{-3}$  s, which provide good converge. High-Order schemes for transient, advective and turbulent terms were used in all simulations with a residual target of  $1 \times 10^{-4}$  (RMS). Unstructured mesh was used in simulations. An Independence mesh test was performed using 70,000; 120,000; 180,000 and 250,000 control volumes. Time-averaged results for pressure drop through the bubble column and velocity profiles of liquid phase showed that 120,000 control volumes are enough to provide results independently of mesh refinement. Figure 2 shows the unstructured mesh used in this case. Mean bubble diameter of 4 mm was used in all cases. Thus it was used in numerical validation of experimental data.

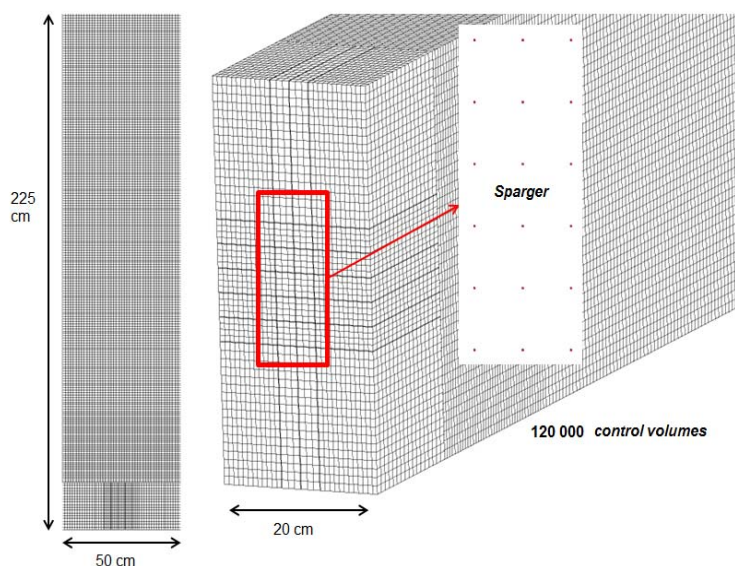


Figure 2: Unstructured mesh (front and bottom view of bubble column).

#### 4. Results and Discussion

The PIV technique was applied to obtain data of velocity field, stress tensors and turbulent kinetic energy. The experimental results provide a general description about gas-liquid flow behaviour in bubble columns for different operating conditions. The gas flow rate was adjusted to yield superficial gas velocities of  $0.05 \text{ cm s}^{-1}$ ,  $0.09 \text{ cm s}^{-1}$ ,  $0.13 \text{ cm s}^{-1}$ . The flow structure in the column cross section was studding at 1.2 m column high. Figures 3a and 3b showing the mean velocity profiles for liquid phase. The  $X_{\text{NORM}}$  coordinate is defined as the  $x$  position divided by half the column width, where  $x = 0$  was considered as the column centre.

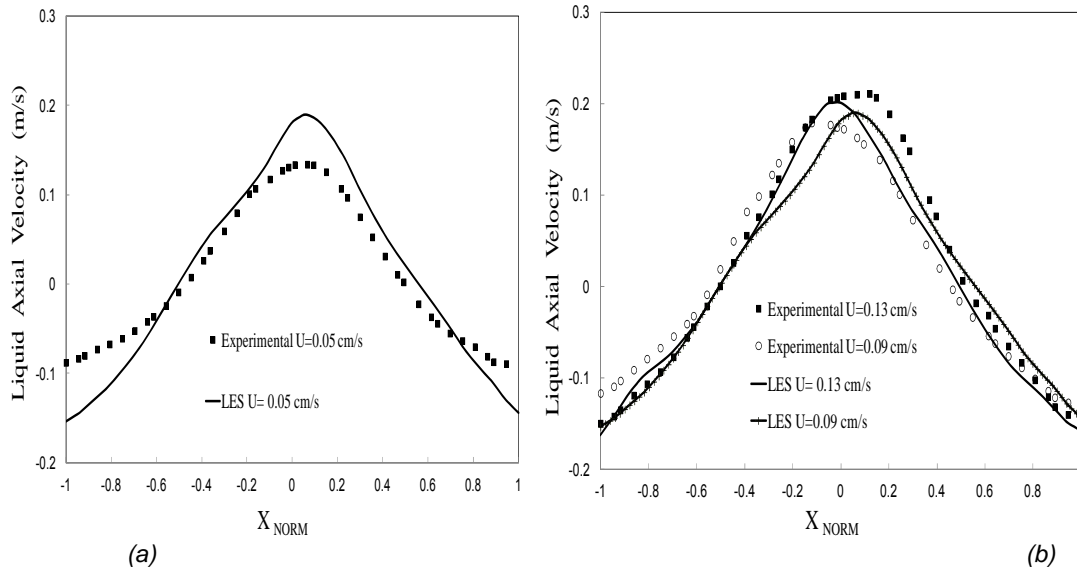


Figure 3: Axial liquid velocity profile - (a)  $u_g = 0.05 \text{ cm s}^{-1}$  (b)  $u_g = 0.09 \text{ cm s}^{-1}$  and  $u_g = 0.13 \text{ cm s}^{-1}$ .

The axial velocity profiles in Figure 3a are parabolic and almost symmetric with vertical component, similarly to that found previously reported by Bröder and Sommerfeld (2009). The symmetry is mainly due to homogeneous dispersion of bubbles across the column. Moreover, the higher local void fraction in the core region will cause the liquid axial velocity to decrease from the centre towards the wall. The experimental data from PIV measurement technique provide reliable detailed data for the validation of numerical simulations.

Figures 3a and 3b show the average axial fluid velocity and the quantitative comparison between experimental data and LES simulation. It can be seen that the model can capture the experimental data reasonably well. This could be explained because LES has ability in capturing the transient central bubble plume movement. Figure 4 shows that the simulation prediction for the highest superficial gas velocity ( $0.13 \text{ cm s}^{-1}$ ) resulted in a better agreement with experimental data. Whereas, for low superficial gas velocity the numerical results tend to overestimates the experimental data. The turbulent kinetic energy ( $k$ ) in the liquid phase induced by the bubbles was calculated by the Albrecht et al. (2002) statistical correlation given by Eq 1:

$$k = \frac{1}{N-1} \left[ \frac{3}{4} (u'_j)^2 + \frac{3}{4} (u'_k)^2 \right] \quad (1)$$

where  $N$  is the number of samples and  $u'$  is the fluctuation of velocity at the  $j$  and  $k$  directions.

Figure 4 shows the turbulent kinetic energy variation along the column width. It has been seen that by increasing the gas superficial velocity will increase the turbulent kinetic energy of the system. This phenomenon is due to the great amount of bubbles into the flow (Bröder and Sommerfeld, 2009). The peaks near the core region are the results of the product of the induced turbulence by the maximum gradients of velocity and bubble interactions.

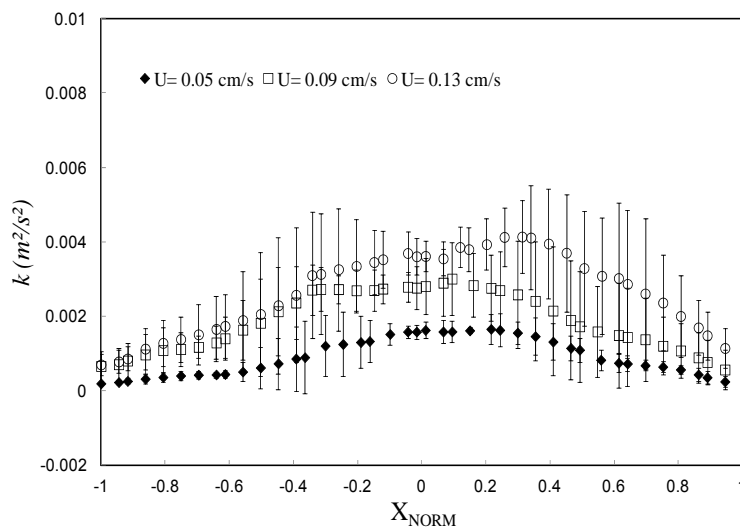


Figure 4: Experimental turbulent kinetic energy profile

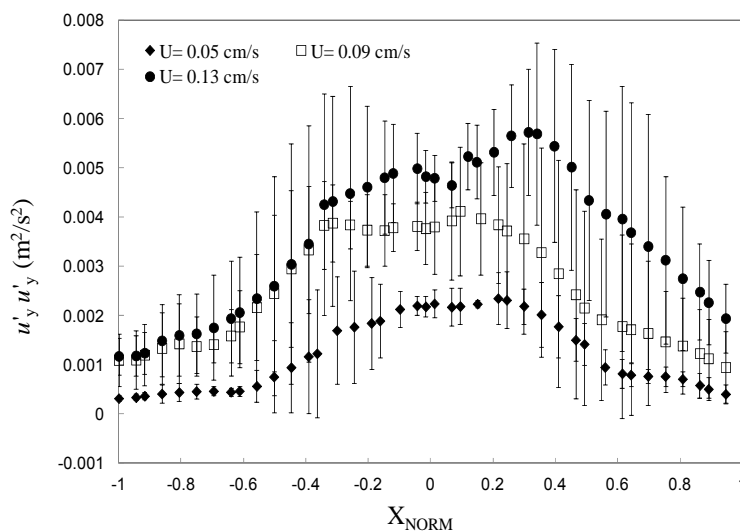


Figure 5: Profile of experimental axial Reynolds stress

The profiles of axial and normal turbulent Reynolds stress of liquid phase are showed in Figures 5 and 6. These profiles represent some characteristics about liquid movement due the bubble motion. The liquid velocity has large fluctuations near the wall ( $X_{\text{NORM}} = 0.3$ ) having upward and downward flow. The Reynolds stress ( $u'_y u'_y$ ) profiles present peaks in this region compared to the centre of the column, where the liquid movement is mainly upward (Figure 6). This behaviour has been found in previously studies (Mudde et al. 1997; Zhou et al. 2002). Otherwise, the oscillatory movements of the bubbles stream through the centre of the column ( $X_{\text{NORM}} \approx 0$ ) leads to the normal Reynolds stress peaks (Figure 6) because the horizontal component of the liquid velocity reaches its highest value at the centre of the column. The difference between normal and axial stress profiles suggests that the turbulence phenomena have an anisotropic behaviour (Mudde et al. 1997; Zhou et al. 2002).

In this work the measurements were performed with confidence intervals of 95 % probability. Analysis of the flow properties (Figures 4, 5 and 6) shows that the largest measurement errors are present near the centre of the column  $X_{\text{Norm}} \approx 0.3$ , where the PIV images are overlapped. Also, the error magnitude of these properties obtained during the evaluation of the flow

characteristics is affected by the intrinsic errors of indirect type measurements (measurements obtained using equations based on measurements taken directly from the equipment).

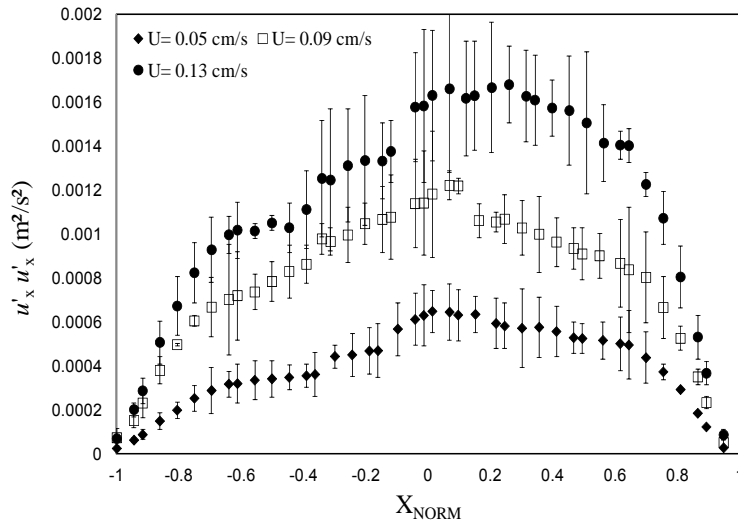


Figure 6: Profile of experimental normal Reynolds stress

## 5. Conclusions

The experiments performed with PIV provided data for fluid dynamics characterization and CFD validation. The experimental results show typical axial velocity profiles of the liquid, upward flow in the core region and a down-flow near the wall due the flow inversion in  $X_{\text{Norm}} \approx 0.5$ . The experimental Reynolds stress profiles show some characteristics about liquid movement due the bubble motion and the difference between normal and axial stress profiles suggests that the turbulence phenomena have an anisotropic behaviour. In the numerical simulation it was observed that for this type of aeration Large Eddy Simulation (LES) predicted well the flow behaviour for all velocities investigated in the bubble column.

## References

- Albrecht H.E.; Borys M., Damaschke N., Tropea C. 2002, Laser Doppler and Phase Doppler Measurement Techniques. Springer. Berlin, Germany.
- Bröder D., Sommerfeld M. 2002, An advanced LIF-PIV system for analysing the hydrodynamics in a laboratory bubble column at higher void fractions. *Experiments in fluids*, 33, 826-837.
- Bröder D., Sommerfeld M. 2007, Planar shadow image velocimetry for the analysis of the hydrodynamics in bubble flows. *Meas. Sci. Technol*, 18, 2513-2528.
- Bröder D., Sommerfeld M. 2009, Analysis of hydrodynamics and microstructure in a bubble column by planar shadow image velocimetry. *Ind. Eng. Chem*, 48, 330-340.
- Degaleesan S., Dudukovic M., Pan Y, 2001, Experimental Study of Gas-Induced Liquid Flow Structures in Bubble Columns. *AIChE Journal*, 47, 1913-1931.
- Dionísio R. P., Silva M. K., d'Ávila M. A. Mori M., 2009, Three-dimensional simulation of bubbly flows with different geometrical approaches, *International Review of Chemical Engineering*, 1, 467-473.
- Ishii M., Zuber N. 1979, Drag coefficient and relative velocity in bubbly, droplet or particulate flows. *AIChE Journal*, 25, 843-855.
- Mudde R.F., Groen J.S., Van Den Akker H.E.A. 1997, Liquid velocity field in a bubble column: LDA experiments. *Chemical Engineering Science*, 52, 4217-4224.
- Nogueira S., Sousa R.G., Pinto A.M.F.R.; Reithmüller M.L., Campos J.B.L.M., 2003, Simultaneous PIV and pulsed shadow technique in slug flow: a solution for optical problems. *Experiments in fluids*, 35, 598-609.
- Silva M.K., Mochi V.T., Conceição D.A., d'Ávila M. A., Mori M., 2011, Experimental and Numerical Analysis of a Gas-Liquid Flow Operating in the Heterogeneous Regime. *Chemical Engineering Transactions*, 24, 1447-1452, DOI: 10.3303/CET1124242
- Tomiyama A. 2004, Drag lift and virtual mass forces acting on a single bubble. *Third International Symposium on Two-Phase Flow Modeling and Experimentation*, Pisa, Italy, September 22-24.
- Zhou L.X., Yang M., Lian C.Y., Fan L.-S., Lee D.J. 2002, On the second-order moment turbulence model for simulating a bubble column. *Chemical Engineering Science*, 57, 3269-3281.